

Dielectric Properties of a Faujasite Y as a Function of the Hydration State

A. Abdoulaye,[†] G. Chabanis,[†] J. C. Giuntini,[†] J. Vanderschueren,^{‡,§} J. V. Zanchetta,^{*,†} and F. Di Renzo^{||}

Laboratoire de Physico-chimie de la Matière Condensée, Equipe de Chimie Physique, UMR 5617, Université Montpellier II, Pl. E. Bataillon, F-34095 Montpellier cedex 05, France, Laboratoire de Chimie Macromoléculaire et Chimie, Groupe d'Etudes des Polymères Industriels et de Dosimétrie Appliquée, B6, Institut de Chimie au Sart-Tilman, B4000 Liège, Belgium, and Laboratoire des Matériaux Catalytiques et Catalyse en Chimie Organique, UMR 5618 CNRS-ENSCM, 8, rue de l'Ecole Normale, 34053 Montpellier, France

Received: July 24, 1996; In Final Form: November 11, 1996[®]

The evolution of conduction and polarization phenomena is studied as a function of dehydration temperature (TT varying from 100 up to 400 °C) on a faujasite Y zeolite. The measurements are carried out as a function of frequency at different temperatures. In all cases, the conductivity is ascribed to the migration of cations in large cages involving energies varying from 0.61 to 0.85 eV. Two relaxation domains are observed. It is assumed that they are due to the movement of cations of sites III' and II. The existence of these two domains is confirmed by the technique of the thermally stimulated currents. The spreading domain of relaxation depends on the dehydration state of the zeolite.

Introduction

Zeolites are natural or synthetic inorganic compounds, the remarkable properties of which lead to several applications. Indeed, crystalline and porous aluminosilicates are used in the industry as ionic exchangers, molecular sieves, waste-water cleanup, sequestration of radioactive cations, catalysts or catalyst support. They have been recently used in photochemistry¹ and as electrolytes in galvanic cells.²

The three-dimensional structure of zeolites, due to the linking of SiO₄ and AlO₄⁻ tetrahedrons, confers on them many interesting properties. The lattice is anionic and the presence of cations is, of course, necessary to make the network neutral. The structure features channels, cages, and windows with dimensions close to those of organic molecules. These void volumes allow the migration of cations or of small molecules adsorbed in the zeolite. The properties and the complexity of the structure of zeolites are at the origin of several works, especially in IR spectroscopy,^{3,4} X-ray diffraction,^{5–9} and NMR.¹⁰ It is an industrial and research domain in full development.

The dielectric properties of these solids have also been studied when gas adsorption is involved, particularly in the case of water vapor.^{11–15} The electrical conductivity of dehydrated zeolites is generally ascribed to exchangeable cations,^{2,11,16–21} and attempts of modeling have been proposed. For example Tabourier et al.²¹ developed a model based on the existence of correlated motion of cations in a "cluster", but there is no complete satisfying model explaining the hopping mechanism. Particularly, the exact nature of the sites concerned with the conduction phenomenon is not really known.

Several interrogations still remain in the study of hydrated or partially hydrated zeolites related to the nature of the carriers

responsible for the hopping conductivity. According to some authors,^{12,15,22} the water molecules can increase the mobility of extraframework cations, while others attribute part of the increase of conductivity to the protons due to the water.^{14,20} However, zeolites are very complex systems and their properties depend on several parameters such as (1) the chemical composition that gives the ratio Si/Al, (2) the type of exchangeable cations, (3) the hydration state or the outgassing temperature, and (4) the measuring temperature. All these parameters affect the distribution of the exchangeable cations on the different sites of the zeolites.

The present work is a contribution to the study of the dielectric properties of zeolites during their dehydration. The study has been performed on a faujasite Y outgassed at different temperatures, taking into account the well-known structure of this zeolite thanks to many studies conducted using X-ray diffraction and Raman and IR spectroscopies.^{3–10} Two techniques have been used in order to analyze the movement of the cations: the complex impedance spectroscopy and the thermally stimulated currents (TSC). We will see that the coupling of these two techniques gives more precise information on the understanding of these media, particularly on the origin of the dielectric properties i.e., the movement of the particles responsible for the electrical transport.

Experimental Methods

The chemical composition of the sample²³ corresponds to a ratio Si/Al = 2.12. This leads to the possible presence of 61 exchangeable cations per unit cell (u.c.). This result has been confirmed by microprobe measurements of ratios Na/(Si + Al) = 0.329 and Al/(Si + Al) = 0.321. The corresponding formula would be Na₆₁(AlO₂)₆₁(SiO₂)₁₃₁·x(H₂O). The crystallinity of the sample has been verified by X-ray powder diffraction.

Zeolite powder is compacted under a pressure of 2.5 × 10⁸ Pa in the form of pellets of 13 mm in diameter and 1.2 mm in thickness. The compactness of the sample is found to be 0.87. Electric contacts are deposited by sputtering a platinum film on the surface of the pellet. To measure the polarization conductivity, a measuring cell is used allowing measurement

* To whom correspondence should be addressed.

[†] Université Montpellier II.

[‡] Institut de Chimie au Sart-Tilman.

[§] Research Associate of the National Fund for Scientific Research (Belgium).

^{||} Laboratoire des Matériaux Catalytiques et Catalyse en Chimie Organique.

[®] Abstract published in *Advance ACS Abstracts*, February 1, 1997.

under vacuum. The setup is assimilated to an equivalent electrical circuit represented by a resistance and a capacitance in parallel.²⁴

The sample was equilibrated at a relative humidity of 48%. It is heated under vacuum (1 Pa) at different outgassing temperatures (TT) varying from 100 up to 400 °C by 50 °C steps and maintained at the chosen temperature for 24 h.

The conductivity measurements are made under vacuum as a function of frequency at different temperatures that obviously cannot exceed TT. The application of a sinusoidal electrical field allows the measurement of the real and imaginary parts of the electrical permittivity. They are evaluated by measuring, respectively, the components in phase and the components shifted by 0.5π with regard to the voltage imposed. This is achieved by an analyzer (HP 4191 A) in the frequency range 10–10 Mhz. The input impedance of the analyzer is larger than 10 M Ω , and its sensitivity of 1.2 pF allows an accuracy of 3.5% to be obtained.

TSC experiments have also been performed on the same samples. These experiments were carried out under helium with a TSC/RMA (relaxation map analysis) spectrometer (Solomat type 91000+) covering the temperature range –170 to 400 °C. This method is described in detail elsewhere.^{26–28} We give here some indications of the principle of the thermally stimulated depolarization current (TSDC) method.

The TSDC method consists of determining, following a strictly controlled temperature program, the current created by the return to an equilibrium state of a dielectric that has been previously polarized. The following steps of polarization and depolarization are generally required when the relaxation spectrum of a material is wanted in a temperature range $T_p - T_0$:

- (i) heating to the polarization temperature T_p
- (ii) application of a dc electric field E_p for a time t_p long enough to obtain saturation of the various polarization process involved
- (iii) rapid cooling in the field to the temperature T_0
- (iv) cutting off the external field and linear heating of the short-circuited sample

The TSDC spectrum (i.e., current induced by depolarization of the sample during heating) is observed during this last step.

In practice, unless otherwise specified, we have adopted T_p values much lower than TT so that the water content of the sample is not significantly affected during the TSDC technique run. Other experimental parameters are $t_p = 2$ min, $T_0 = -160$ °C, $E_p = 3 \times 10^5$ V/m, and the heating rate, b , being 10 °C/min⁻¹.

The method of thermally stimulated polarization current (TSPC) is the natural complement of the TSDC technique. It is based on the opposite process, i.e., measuring the currents generated by the buildup of the polarized state in a dielectric (external field applied during heating). It has been used to check the intrinsic nature of the relaxations observed.

These TSDC and TSPC methods are “global” techniques allowing a complete picture of the temperature-dependent relaxations to be observed in one experiment. Their performances can be further markedly increased when used in a fractional analytical mode (relaxation map analysis, RMA), allowing progressive isolation of a series of subrelaxations corresponding to quasi-elementary motions.^{26,27}

To analyze specific regions of the TSDC spectrum, all these methods were used to some extent, namely, TSDC and TSPC global experiments as well as thermal windowing experiments for RMA analysis. Blocking electrodes (10 μ m thick Teflon foils) were used for avoiding electrode polarization and injection effects.

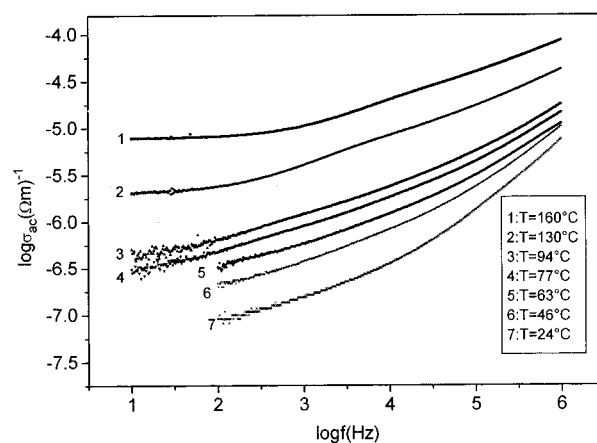


Figure 1. Variation of the total conductivity, σ_{ac} , as a function of frequency at different temperatures of measurement (TT = 400 °C).

It has already been shown that the techniques of polarization conductivity and of the TDSC are complementary.^{11,13,29,30}

Results and Discussion

Direct Current Conductivity. The typical variation of the total ac conductivity, determined as a function of frequency f ($\omega = 2\pi f$) is reported in Figure 1, which shows, as an example, the conductivity of a faujasite for different measuring temperatures and characterized by the outgassing temperature TT = 400 °C. Some results are reported at lower frequency showing a dispersion of the experimental results due to the characteristics of the sample. The total conductivity takes the form

$$\sigma_{ac}(\omega) = \sigma_0 + \sigma'(\omega)$$

where σ_0 is the limit of the conductivity when $\omega \rightarrow 0$. It is well-known that this part, independent of frequency, is related to the dc conductivity and that $\sigma'(\omega) = A\omega^s$, is the dispersive part, which is predominant above a given value of frequency. This decomposition can be seen easily when measurements are performed at high temperatures. The law $A\omega^s$ has been observed on disordered solids in general and more precisely on electronic and ionic semiconductors. It has been called the “universal law” by Jonscher.^{31,32} The exponent s , which is a function of temperature and frequency,^{33,34} varies generally from 0 to 1, and parameter A depends on temperature.^{35–37} For relatively high measuring temperatures ($T \geq 150$ °C for TT = 400 °C) the dc conductivity, σ_0 , can be determined. Following the usual phenomenology, this component is ascribed to the movement of free charges.^{29,37} Indeed, under the influence of an electrical field, there is an appearance of current density that creates long distance carriers movements. This is generally called diffusion current. On the present samples, we found that σ_0 verifies the Arrhenius law for all outgassing temperatures TT:

$$\sigma_0 = \frac{B}{T} \exp\left(-\frac{E_{dc}}{kT}\right)$$

where E_{dc} is the corresponding activation energy, B is the preexponential factor containing the number of carriers and the hopping distance, and k is the Boltzmann constant. This equation expresses the Nernst–Einstein relation, which connects the conductivity to the diffusion coefficient of the carrier, assuming that a thermally activated three-dimensional hop takes place.³⁸ The Arrhenius diagrams are reported in Figure 2 for different TT. For low TT, the thermal domain of study is, of course, reduced (the measuring temperature has to be lower or the more equal to TT). Moreover, at low temperature the values

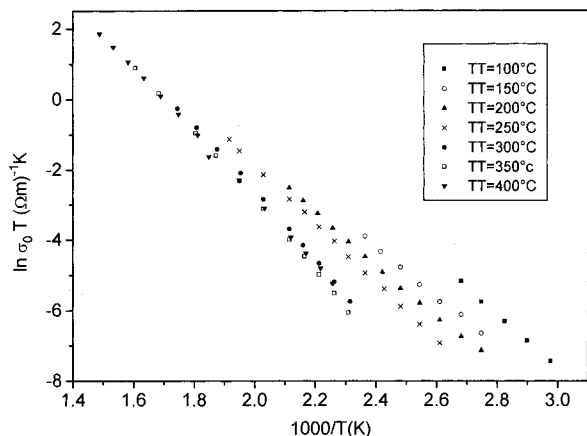


Figure 2. Arrhenius plots of the dc conductivity at different TT.

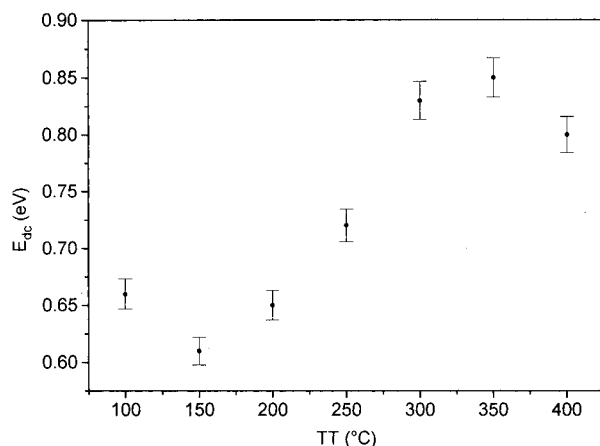


Figure 3. Variations of E_{dc} with TT.

of σ_0 are too small to be measurable. The different values of E_{dc} are reported in Figure 3 for different values of TT. It can be observed that there is a decrease of the activation energy in the domain 100–150 °C, and then E_{dc} increases regularly and decreases again slightly for TT > 350 °C.

It is actually accepted that the faujasite Y is anhydrous when it is outgassed at 400 °C under vacuum for at least 12 h.^{3,4,16,22,39,40} For partially dehydrated samples, “free water” is still present as confirmed by IR spectroscopy and thermogravimetric analysis.^{3,4} The cations are distributed between large cages (α -cages) and small cages (sodalite cages or β -cages and hexagonal prisms). The cations in large cages are surrounded by “free water”. They are very mobile and contribute to the dc conductivity. The decrease of E_{dc} between 100 and 150 °C could be explained by considering that at 100 °C some acceptor sites are still occupied by water molecules. The occupation of such sites by hopping cations would be related to the rupture of hydrogen bonds during the conduction. It can be assumed that Na^+ ions form water entities such as $[\text{Na}(\text{H}_2\text{O})_x]^+$, the displacement of which would require more energy.⁷ At 150 °C, these entities break up and the cations become localized, which explains the increase of the observed activation energy in the conduction process beyond this temperature. This water disappears near 250 °C,^{3,4} creating a strong decrease of the cation mobility in large cages and therefore a decrease of the conductivity as shown in Figure 4. This figure represents the evolution of the dc conductivity at 150 °C for different TT. There is a sharp variation between TT = 250 and 300 °C. Indeed, at 300 °C there is no more water in the supercages, and the few remaining water molecules are localized in the sodalite cages where they are strongly bound.^{7,41,42} Therefore, they have little influence on the mobility of the cations in the

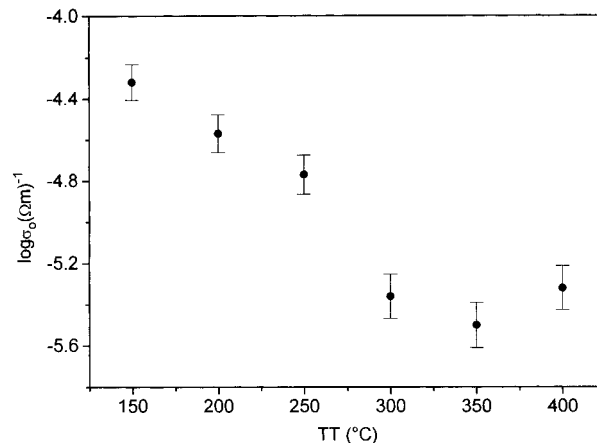


Figure 4. Evolution of the dc conductivity, σ_0 , measured at 150 °C for different TT.

large cages. The cations in the small cages are not directly involved in the conduction phenomenon.

The value of $E_{dc} = 0.80$ eV found on the anhydrous sample is close to that of 0.77 eV reported by Carru et al.²² for a ratio Si/Al = 2.4. This value is in agreement with those found on faujasites, with typical values of 0.74 eV for Si/Al = 1.75 and 0.84 for Si/Al = 2.51.⁴⁰

Relaxation. Alternating Current Conductivity. As already mentioned, for a given frequency, the component $\sigma'(\omega) = A\omega^s$ is predominant as shown in Figure 1. This phenomenon is increased when the temperature decreases. This polarization phenomenon is related to cationic relaxation due to limited movements of exchangeable cations. It is therefore ascribed to local movements ascribed to the hops of ions near their equilibrium positions. The charge carriers responsible for this phenomenon are usually called “bound charges”.^{29,32,33} In the kilohertz region, two relaxation domains have been found by authors near room temperature on dehydrated faujasites^{40,43,44} and on hydrated or partially hydrated zeolites.^{45,46} However, these two relaxations are not ascribed to the same species, depending on authors. Thus, Matron et al.⁴⁴ ascribed the two relaxations observed on dehydrated zeolites to cations in different sites, while Jansen et al.⁴⁰ refer to a Maxwell–Wagner effect at low frequency and to cationic relaxation at high frequency. On hydrated zeolites, the two relaxations have been ascribed to cations, to water molecules, or to Maxwell–Wagner effects.^{44,45} This last hypothesis will not be considered in the present work, since the arguments are not particularly convincing. Moreover, the Cole–Cole plots are not characteristic of such an effect.

Figure 5 reports the total conductivity $\sigma_{ac}(\omega)$ for different TT, the measuring temperature being 63 °C. Considering the frequency domain and the temperature of measurement, $\sigma_{ac}(\omega)$ can be assimilated to $\sigma'(\omega)$. In this figure a peak (see the arrows in Figure 5), which moves toward low frequencies when TT increases, can be identified. We have considered two relaxation regimes on both sides of the peak: a low-frequency relaxation (LF) corresponding to relatively high energies and a high-frequency relaxation (HF) implying weaker energies. For example, for TT = 250 °C, the HF relaxation is characterized by an activation energy of 0.38 eV and the LF relaxation by 0.56 eV. The two regimes are clearly identified from Arrhenius plots as reported in Figure 6 (TT = 250 °C, $\log f = 4$ for LF, and $\log f = 5.5$ for HF).

When the outgassing temperature, TT, increases (for a given temperature of measurement), the intensity of the LF relaxation decreases and the relaxation moves to lower frequencies and

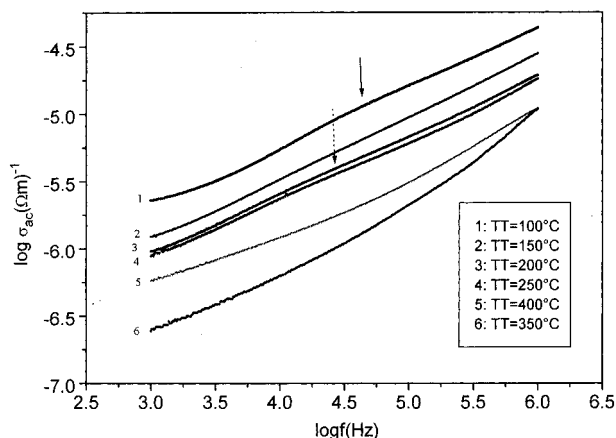


Figure 5. Plots of $\sigma_{ac} = f(\text{frequency})$ for $T = 63\text{ }^{\circ}\text{C}$ showing two relaxation regions. The arrow indicates the peak separating the regimes of relaxation.

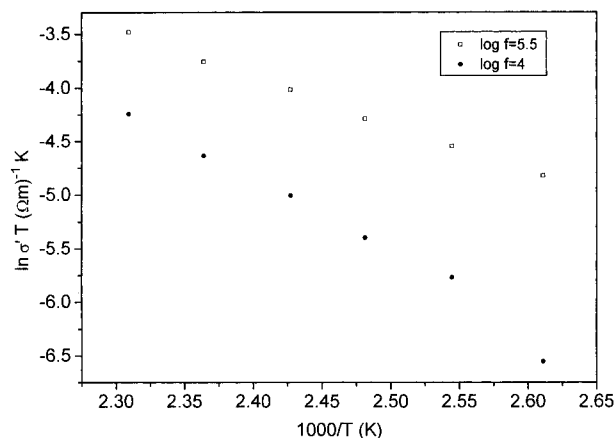


Figure 6. Evolution of the polarization conductivity for two frequencies corresponding to the two relaxation regimes as a function of the reciprocal measuring temperature.

disappears when TT reaches $350\text{ }^{\circ}\text{C}$. Therefore, a sole relaxation peak remains, the position of which moves slowly toward the low-frequency region. These two relaxations can be ascribed to cations located in sites energetically different. It is known that in faujasite Y the cations become more and more localized when the dehydration temperature increases,^{7,46,47} and consequently, their mobility decreases. Thus, at low outgassing temperatures TT, the thermal motion, determined by the measuring temperature, allows the excitation of two types of carriers. When dehydration takes place, the charge carriers responsible for the LF relaxation can hardly be oriented. As a consequence, in the anhydrous zeolite, only the cation movement responsible for the HF relaxation is detected. The corresponding activation energy is 0.40 eV . To observe the LF relaxation, we have performed high-temperature measurements. Figure 7 shows the evolution of the two relaxations at $TT = 350\text{ }^{\circ}\text{C}$. For partially dehydrated states ($100\text{ }^{\circ}\text{C}$ for example), if we accept that cations are in a kind of liquid phase called “mobile phase”, similar to an electrolyte solution,^{7,48} they likely are localized in the large cages, more precisely in sites III' and II.⁷ During dehydration, the “mobile phase” disappears and the migration of cations toward sites II takes place.^{7,48} Based on a X-ray measurements,^{7,45,47} the number of the cations in sites II goes from $16\text{ Na}^+/\text{u.c.}$ in the hydrated state to $28\text{ Na}^+/\text{u.c.}$ in the anhydrous state while the rate of occupation of sites III' is weak.

During dehydration, the energy necessary to move the cations from sites II increases, and only the cations of sites III' are involved, being less strongly bound to the oxygen atoms of the

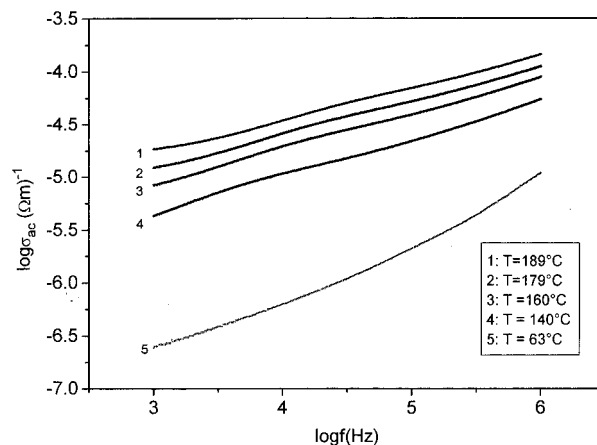


Figure 7. Evolution of the two relaxation regions as a function of the measuring temperature ($TT = 350\text{ }^{\circ}\text{C}$).

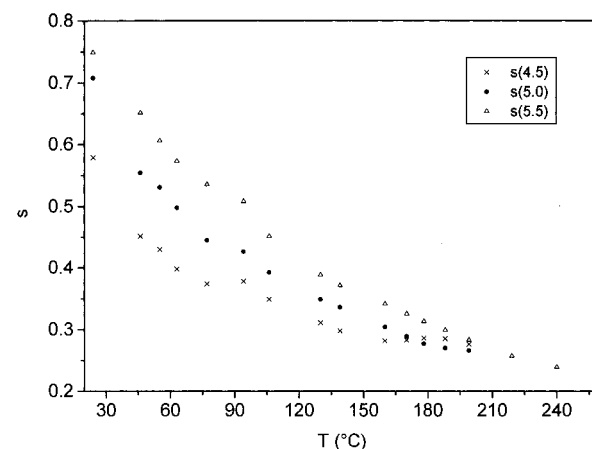


Figure 8. Temperature dependence of parameter s ($TT = 400\text{ }^{\circ}\text{C}$) at different frequencies ($\log f = 4.5, 5$, and 5.5).

network.^{22,49} The cations of sites II are more strongly coordinated to the oxygen atoms of the network,^{5,7,9,40} which explains the decrease of the intensity of the two relaxations (LF and HF) and the displacement of the LF relaxation toward high energy when outgassing.

These considerations lead us to ascribe the LF relaxation to cations in sites II and the HF relaxation to cations in sites III' of the supercages. These relaxations correspond to hops of cations in neighboring sites. Thus, the intensity decrease of relaxation HF with TT (up to $350\text{ }^{\circ}\text{C}$) is explained both by the localization of the cations in sites III' and by the reduction of their number. Between $350\text{ }^{\circ}\text{C}$ and $400\text{ }^{\circ}\text{C}$, the small modification of the behavior of the conductivity can be explained by a small increase of the carrier number in sites III'. The single relaxation on the sample at $TT = 400\text{ }^{\circ}\text{C}$ for low-temperature measurements, and characterized by an activation energy of 0.40 eV , is ascribed to cations of sites III'. This result is consistent with the interpretation of Jansen et al.⁴⁰ These authors have interpreted the observed relaxation on a series of faujasites (near room temperature) as a cationic relaxation of sites III' characterized by energies varying from 0.31 to 0.44 eV . The HF relaxation observed by Matron et al.⁴⁴ corresponds to an energy of 0.42 eV .

The dispersive part of the conductivity $\sigma'(\omega) = A\omega^s$ leads to the determination of parameter s . Figure 8 shows the temperature dependence of exponent s at different frequencies for $TT = 400\text{ }^{\circ}\text{C}$, which is an example. These determinations are performed at high frequency in order to avoid the influence of the dc conductivity. This parameter is a decreasing function of temperature and is practically constant for $T \approx 250\text{ }^{\circ}\text{C}$. The

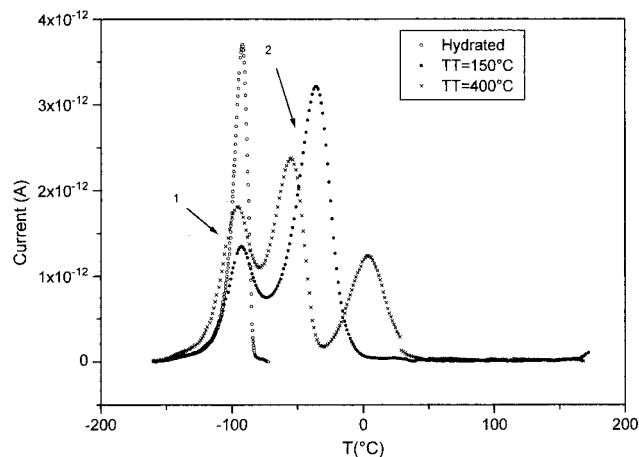


Figure 9. TSDC spectra for different TT ($E_p = 3 \times 10^5 \text{ V m}^{-1}$; $t_p = 2 \text{ min}$; $T_0 = -160^\circ\text{C}$; $b = 10^\circ\text{C min}^{-1}$; (O) $T_p = 0^\circ\text{C}$; (●, ×) $T_p = 150^\circ\text{C}$).

decrease of s reflects the increasing disorder of the solids.¹⁸ It can be seen that s increases with frequency as already seen in the case of totally different compounds.³⁴

TSDC Measurements. The interpretation proposed on the basis of the ac conductivity measurement is supported by the TSC measurements.

In Figure 9, the TSDC curves obtained for TT = 150 and 400 °C ($T_p < TT$) are compared to that obtained for hydrated samples (i.e., samples previously kept in 48% relative humidity and not outgassed). In this last case, the polarization temperature T_p was maintained at 0 °C in order to avoid any possible dehydration during the TSC runs. It has also been checked that in blocking conditions, the current density is always proportional to the applied field and that the TSDC and TSPC peaks are strictly identical (position, height, and shape), the only difference being that they obviously appear in opposite directions (i.e., they are mirror images from one another). These facts strongly suggest that the underlying polarization and depolarization processes involve only local, dipolar-like motions.^{26,27,29}

In materials that are not outgassed, only one peak is observed in the temperature range investigated (-160 to 25°C). It corresponds to cations localized in supercages and creating dipoles that can be oriented. After outgassing, this peak is split in two components (1 and 2 in order of increasing temperatures), probably corresponding to the localization of the cations in sites III' and II, respectively. From windowing experiments and RMA analysis,^{26,27,29} the distributions of activation energies have been determined. Peak 1, of weak intensity, corresponds to maximum energies of 0.49 and 0.46 eV for TT = 150 and 400 °C, respectively. Peak 2, of higher intensity, corresponds to maximum energies of 0.67 and 0.54 eV for the same respective TT.

When TT increases, peaks 1 and 2 become closer, which reflects, especially for the high temperature of the measurements, a migration of cations from sites II to sites III'. This result has to be compared to the behavior of the dc conductivity of the anhydrous zeolites. This hypothesis was already proposed by Jansen et al.⁴⁰ from conductivity measurements on similar compounds.

In the TT interval 150–400 °C, a third type of carrier, activated by higher energies, appears (see in Figure 9 the TSDC peak located near 10°C). It corresponds to cations localized either in sodalite cages or in hexagonal prisms. The occupancy level of these prisms (sites I) is very small and sometimes negligible.^{7,42} Therefore, this peak corresponds probably to cations in sites I' in the sodalite cages. The charge carriers in these

sites are strongly bound when the zeolite is partially dehydrated. Some authors claim, in this context, that there is a direct coordination of the cations with the negative charges of the surface of the zeolite.^{42,44} In accordance with this assumption the cations of this region of the zeolite structure form ion pairs with the negative charges of the zeolite and therefore can hardly be resited. They do not participate in the relaxation process, considering the frequency and temperature domains used in the present impedance spectroscopy experiments.

When TT increases, peaks 1 and 2 become nearer, which indicates, especially for the high temperatures of the measurement, the migration of the cations from sites II to sites III' and explains the dc conductivity in anhydrous zeolites. This hypothesis was previously proposed by Jansen et al.⁴⁰ from conductivity measurements on similar compounds.

The population of sites in the small cavities is practically not modified by dehydration.^{7,50} The corresponding energy (i.e., the energy of the carrier trapped in its site) varies with the hydration state; it is relatively high in the hydrated state, since there is a stabilization effect of the water molecules localized in the sites II'.⁵¹

Conclusion

The dielectric properties of a faujasite Y have been studied as a function of temperature for different levels of dehydration. The evolution of these properties are strictly connected with the outgassing temperature, the variations being particularly clear beyond 250°C . The highest conductivity is observed on a sample outgassed at 100°C and the highest resistivity after degassing at 350°C . All the results confirm this behavior (σ_0 , σ_{ac} , and E_{dc}).

For all outgassing temperatures, the samples present two relaxation regions, the importance of which depends on the measuring temperature, i.e., on the thermal motion of the system. In all cases, these two relaxation domains are ascribed to cations in sites III' and II of the large cages. The LF relaxation is attributed to cations of sites II and the HF relaxation to cations of sites III'. Only the cations of site III' remain at relatively low measuring temperatures in anhydrous samples. The conduction and the polarization process occur through cations hops (on more or less large distances) between neighboring sites.

The TSC measurements confirm most of the conclusions of the impedance investigations. The clear separation of the TSDC peaks indicates undoubtedly the localization of the cations in sites II and III' and leads to the evaluation of the corresponding energies. Owing to its high sensitivity, this technique also allows the cations of the sodalite cage to be detected. Generally speaking, the TSC method appears as an alternative method complementary to the impedance spectrometry measurements.

References and Notes

- (1) Hepp, M. A.; Ramamurthy, V.; Corbin, D. R.; Dybowski, C. J. *Phys. Chem.* **1992**, 96, 2629.
- (2) Vigil, O.; Heredia, H.; Leccabue, F.; Watts, B. E. *Phys. Status Solidi. A* **1993**, 135, K71.
- (3) Ward, J. W. *J. Phys. Chem.* **1963**, 72 (12), 4211.
- (4) Angell, C. L.; Schaffer, P. C. *J. Phys. Chem.* **1963**, 69 (10), 3463.
- (5) Mortier, W. J.; Bosmans, H. J. *J. Phys. Chem.* **1971**, 75 (21), 3327.
- (6) Olson, D. H. *J. Phys. Chem.* **1970**, 74 (14), 2758.
- (7) Beagly, B.; Dwyer, J.; Fitch, F. R.; Zanjanchi, M. A. *J. Inclusion Phenom.* **1985**, 3, 143.
- (8) Klein, H.; Kirschhock, C.; Fuess, H. *J. Phys. Chem.* **1994**, 98, 1245.
- (9) Olson, D. H. *Zeolites* **1995**, 15, 439.
- (10) Melchior, M. T.; Vaughan, D. E. W.; Pictroski, C. F. *J. Phys. Chem.* **1995**, 99, 6128.
- (11) Sousa Gonçalves, J. A.; Portsmouth, R. L.; Alexander, P.; Gladden, L. F. *J. Phys. Chem.* **1995**, 99, 3317.
- (12) Pissis, P.; Diamanti, D. D. *J. Phys. Chem. Solids* **1993**, 54 (6), 701.
- (13) Stamires, D. N. *J. Chem. Phys.* **1962**, 36 (12), 3174.

- (13) Chabanis, G.; Mouton, V.; Abdoulaye, A.; Giuntini, J. C.; Zanchetta, J. V. *Ionics* **1995**, *1* (2), 177.
- (14) Andersen, E. K.; Andersen, I. K.; Skou, E.; Andersen, S. Yde. In *Solid State Protonic Conductors III*; Odense University Press: Odense, Denmark, 1985.
- (15) Rabinowitsch, E.; Wood, W. C. Z. *Elektrochem.* **1933**, *39*, 562.
- (16) Freeman, D. C.; Stamires, D. N., Jr. *J. Chem. Phys.* **1961**, *35*, 799.
- (17) Ohgushi, T. *Bull. Chem. Soc. Jpn.* **1988**, *61*, 1109.
- (18) Vigil, O.; Fundora, J.; Leccabue, F.; Watts, B. E. *Phys. Status Solidi A* **1994**, *141*, K37.
- (19) Kelemen, G.; Schön, G. *J. Mater. Science* **1992**, *27*, 6036.
- (20) Mongensen, N. H.; Skou, E. *Solid State Ionics* **1995**, *77*, 51.
- (21) Tabourier, P.; Carru, J. C.; Wacrenier, J. M. *J. Chim. Phys. Phys.-Chim. Biol.* **1990**, *87*, 43.
- (22) Carru, J. C.; Tabourier, P.; Wacrenier, J. M. *J. Chim. Phys. Phys.-Chim. Biol.* **1991**, *88*, 307.
- (23) Di Renzo, F.; Fajula, F.; Figueras, F.; Nicolle, M. A.; Courières, T. Des In *Synthesis of Microporous Materials*; Occelli, M. L., Robson, H., Eds.; Van Nostrand Reinhold: New York, 1992; Vol. 1, p 105.
- (24) Giuntini, J. C.; Zanchetta, J. V.; Brach, I.; Diaby, S. *Advanced Methods in Coals Characterization*; Elsevier: Amsterdam, 1990.
- (25) Giuntini, J. C.; Jabobker, A.; Zanchetta, J. V. *Clay Miner.* **1985**, *20*, 347.
- (26) Ibar, J. P. *Fundamentals of Thermally Stimulated Current and Relaxation Map Analysis*; SLP Press: New York, 1993.
- (27) Vanderschueren, J.; Gasiot, J. Field-Induced Thermally Stimulated Currents. In *Thermally Stimulated Relaxation in Solids*; Braunlich, P., Ed.; Topics in Applied Physics 33; Springer-Verlag: Berlin, 1979; Chapter 4.
- (28) Van Turnhout, J. Thermally Stimulated Discharge of Electrets. In *Electrets*; Sessler, G. M., Ed.; Topics in Applied Physics 33; Springer-Verlag: Berlin, 1980; Chapter 3.
- (29) Giuntini, J. C.; Vanderschueren, J.; Zanchetta, J. V.; Henn, F. *Phys. Rev. B* **1994**, *50*, 12489.
- (30) Doi, A. *J. Mater. Sci. Lett.* **1984**, *3*, 613.
- (31) Jonscher, A. K. *Nature* **1977**, *267*, 673.
- (32) Jonscher, A. K. *Dielectric Relaxation in Solids*; Chesla Dielectric: London, 1983.
- (33) Buet, F.; Giuntini, J. C.; Henn, F.; Zanchetta, J. V. *Philos. Mag. B* **1992**, *66* (1), 77.
- (34) Salam, F.; Giuntini, J. C.; Soulayman, S. Sh.; Zanchetta, J. V. *Appl. Phys. A* **1995**, *60*, 309.
- (35) Nowick, A. S.; Lim, B. S.; Vaysleyb, A. V. *J. Non-Cryst. Solids* **1994**, *172-174*, 1243.
- (36) Lee, W. K.; Liu, J. F.; Nowick, A. S. *Phys. Rev. Lett.* **1991**, *67* (12), 1559.
- (37) Lu, X.; Jain, H. *J. Phys. Chem. Solids* **1994**, *55* (12), 1433.
- (38) Slade, R. C. T.; Jinku, H.; Hix, G. B. *Solid State Ionics* **1992**, *57*, 117.
- (39) Tikhomirova, N. N.; Nikoloeva, I. V. *Russ. J. Phys. Chem. (Engl. Transl.)* **1981**, *55* (9), 1265.
- (40) Jansen, F. J.; Schoonheydt, R. A. *J. Chem. Soc., Faraday Trans. 1* **1973**, *69*, 1338.
- (41) Sherry, H. S. *J. Phys. Chem.* **1966**, *70* (4), 1158.
- (42) Sherry, H. S. *J. Phys. Chem.* **1968**, *72* (12), 4086.
- (43) Lhose, U.; Stach, H.; Hollnagel, M.; Schirmer, W. *Monatsberichte der Deutschen Akademie der Wissenschaften zu Berlin*; Akademie-Verlag: Berlin, 1970; Vol. 12, p 819.
- (44) Matron, W.; Ebert, G.; Müller, F. H. *Kolloid Z. Z. Polym.* **1971**, *248*, 986.
- (45) Lhose, U.; Stach, H.; Schirmer, W. *Z. Phys. Chem.* **1973**, *254*, 59.
- (46) Schoonheydt, R. A.; De Wilde, W.; Velghe, F. *J. Phys. Chem.* **1976**, *80* (5), 511.
- (47) Costenoble, M. L.; Mortier, W. J.; Uytterhoeven, J. B. *J. Chem. Soc., Faraday Trans. 1* **1976**, *72*, 1877.
- (48) Barrer, R. M.; Walker, A. J. *Trans. Faraday Soc.* **1964**, *60*, 171.
- (49) Dempsey, E. *J. Phys. Chem.* **1969**, *76*, 3660.
- (50) Eulenberger, G. R.; Shoemaker, D. P.; Keil, J. G. *J. Phys. Chem.* **1967**, *71* (6), 1812.
- (51) Van Dun, J. J.; Mortier, W. J. *J. Phys. Chem. Solids* **1989**, *50*, 469.